The Role of Toroidal and Cylindrical Chemical Bonding Manifolds in Coinage Metal and Mercury Clusters†

R. B. King
Department of Chemistry, University of Georgia, Athens, Georgia 30602

Received May 18, 1993®

The coinage metals (copper, silver, gold) and mercury in their cluster compounds frequently do not use a three-dimensional nine-orbital sp^3d^5 spherical bonding manifold but instead either a two-dimensional eight-orbital sp^2d^5 toroidal bonding manifold or a one-dimensional seven-orbital spd^5 cylindrical bonding manifold. The antibonding p orbitals of the toroidal and cylindrical bonding manifolds can receive electron density from the filled d orbitals of adjacent metal atoms through $d\sigma \rightarrow p\sigma^*$ and/or $d\pi \rightarrow p\pi^*$ back-bonding, leading to bonding distances between adjacent metal atoms. Coinage metal clusters with toroidal and/or cylindrical bonding manifolds include centered gold clusters as well as polynuclear coinage metal alkyls, aryls, and alkynyls. Mercury clusters of interest include the cluster anions in alkali metal amalgams, clusters containing transition metal macropolygons or macropolyhedra with M–Hg–M edges and linear mercury atoms, and clusters containing either one or two mercury atoms sandwiched between Pt_3 or Pd_3 triangles.

INTRODUCTION

The accessible spd valence orbital manifold of most transition metals consists of nine orbitals (sp^3d^5) and has spherical (isotropic) geometry extending equally in all three dimensions, where the geometry of an orbital manifold relates to contours of the sum $\sum\psi^2$ over all orbitals in the manifold. Filling this accessible spherical spd manifold with electrons from either the central metal atom or its surrounding ligands results in the familiar 18-electron configuration of the next rare gas.

A specific feature of the chemical bonding in some systems containing the late transition and early posttransition metals observed by Nyholm[1] as early as 1961 is the shifting of one or two of the outer p orbitals to such high energies that they no longer participate in the chemical bonding and the accessible spd valence orbital manifold is no longer spherical (isotropic). If one p orbital is so shifted to become antibonding, then the accessible spd orbital manifold contains only eight orbitals (sp^2d^5) and has the geometry of a torus or doughnut (Figure 1). The "missing" p orbital is responsible for the hole in the doughnut. This toroidal sp^2d^5 manifold can bond only in the two dimensions of the plane of the ring of the torus. Filling this sp^2d^5 manifold of eight orbitals with electrons leading to the 16-electron configuration found in square planar complexes of the d^8 transition metals such as Rh(I), Ir(I), Ni(II), Pd(II), Pt(II), and Au(III). The locations of the four ligands in these square planar complexes can be considered to be points on the surface of the torus corresponding to the sp^2d^5 manifold. The toroidal sp^2d^5 manifold can also lead to trigonal planar and pentagonal planar coordination for three- and five-coordinate complexes, respectively. The x, y, and z axes for a toroidal sp^2d^5 manifold are conventionally chosen so that the missing p orbital is the p_z orbital.

In some structures containing the late transition and posttransition metals, particularly the 5d metals Pt, Au, Hg, and Tl, two of the outer p orbitals are raised to antibonding energy levels. This leaves only one p orbital in the accessible spd orbital manifold, which now contains seven orbitals (spd^5) and has cylindrical geometry extending in one axial dimension much further than in the remaining two dimensions (Figure 1). Filling this seven-orbital spd^5 manifold with electrons leads to the 14-electron configuration found in two-coordinate linear complexes of d^{10} metals such as Pt(0), Cu(I), Ag(I), Au(I), Hg(II), and Tl(III). The raising of one or particularly two outer p orbitals to antibonding levels has been attributed to relativistic effects.

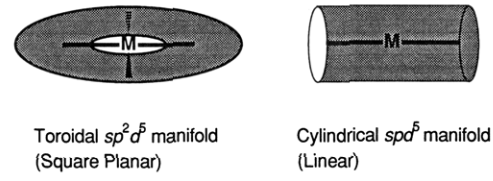

Figure 1. Toroidal sp^2d^5 and cylindrical spd^5 manifolds showing square planar coordination for the toroidal manifold.

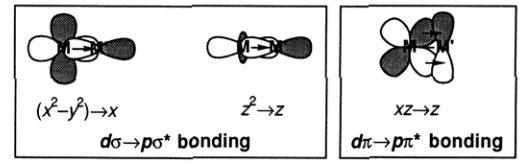

Figure 2. Idealized examples of $d\sigma \rightarrow p\sigma^*$ or $d\pi \rightarrow p\pi^*$ bonding such as that found in coinage metal and mercury derivatives with toroidal and cylindrical valence orbital manifolds.

There are some aspects of mercury chemistry that can be interpreted on the basis of a stable six-orbital sd^5 bonding manifold in which all three outer p orbitals are raised to antibonding energy levels. Since the p orbital set p^3 is isotropic (spherical), the sd^5 bonding manifold is also isotropic. The simplest example of a stable six-orbital sd^5 bonding manifold in mercury chemistry is elemental mercury itself, in which the 12 valence electrons of mercury can exactly fill this sd^5 manifold leading to a "pseudonoble gas" electron configuration. Elemental mercury is far more volatile than any other metal and has a monoatomic vapor similar to the vapors of the noble gases.

The p orbitals which are raised to antibonding levels as noted above can participate in $d\sigma \rightarrow p\sigma^*$ or $d\pi \rightarrow p\pi^*$ bonding in complexes of metals with toroidal sp^2d^5, cylindrical spd^5, and spherical sd^5 manifolds, depending on the symmetry of the overlap (Figure 2). Such bonding has been suggested by Dedieu and Hoffmann[2] for Pt(0)–Pt(0) dimers on the basis of extended Hückel calculations. This type of surface bonding like, for example, the $d\pi \rightarrow p\pi^*$ back-bonding in metal

† Paper presented at the Fifth International Conference on Mathematical and Computational Chemistry, Kansas City, MO, May 1993.
® Abstract published in *Advance ACS Abstracts,* February 15, 1994.

0095-2338/94/1634-0410$04.50/0

carbonyls, does not affect the electron bookkeeping in the late transition and posttransition metal clusters but accounts for the bonding rather than nonbonding distances between adjacent metal vertices in such clusters.

This paper examines the role that eight-orbital toroidal sp^2d^5 and seven-orbital cylindrical spd^5 valence orbital manifolds play in the structure and bonding in clusters of the coinage metals and mercury. Coinage metal clusters treated in this paper include gold clusters, coinage metal alkyls and aryls, and both homonuclear and heteronuclear coinage metal alkynyl derivatives. Mercury clusters treated in this paper include the cluster anions in alkali metal amalgams as well as transition metal clusters of various types containing mercury.

COINAGE METAL CLUSTERS

A. Centered Gold Clusters. An important class of gold clusters includes the *centered* gold clusters.[3] Such clusters containing n gold atoms consist of a central gold atom surrounded by $n-1$ peripheral gold atoms. The peripheral gold atoms all have a seven-orbital cylindrical spd^5 manifold of bonding orbitals and can be divided into the following two types: (1) belt gold atoms which form a puckered hexagonal or octagonal belt around the center gold atom; (2) distal gold atoms which appear above or below the belt gold atoms. The topology of the centered gold clusters can be considered to be either spherical or toroidal, depending on whether the center gold atom uses a nine-orbital spherical sp^3d^5 manifold or an eight-orbital toroidal sp^2d^5 manifold of bonding orbitals. This distinction between spherical and toroidal centered gold clusters was first recognized by Mingos and co-workers.[4] Centered gold clusters have also been described as "porcupine compounds" since the central gold atom corresponds to the body of the porcupine and the peripheral gold atoms (with cylindrical geometry as noted above) correspond to the quills of the porcupine.[5]

The following features of centered gold clusters make their systematics very different from other metal cluster compounds such as metal carbonyl clusters:

(1) The volume enclosed by the peripheral gold atoms must be large enough to contain the center gold atom. Thus the volume of a cube of eight peripheral gold atoms is not large enough to contain a ninth center gold atom without some distortion. Therefore centered cube gold clusters of the stoichiometry $Au_9L_8^+$, such as $Au_9(PPh_3)_8^+$ (ref 6), are distorted from the ideal O_h symmetry to lower symmetry such as D_3. However, the volume of an icosahedron of 12 peripheral gold atoms is large enough to contain a thirteenth central gold atom without any distortion, as shown by the structure[7] of $Au_{13}Cl_2(PMe_2Ph)_{10}^{3+}$. The peripheral gold polyhedron of a spherical gold cluster containing fewer than 13 total gold atoms is generally based on an undistorted icosahedral fragment which has a large enough volume for the center gold atom.

(2) The overlap topology at the core of a centered Au_n cluster from the $n-1$ unique internal orbitals of the peripheral gold atoms is not that of a K_{n-1} complete graph as in other globally delocalized metal clusters.[8-13] Instead the overlap topology of the unique internal orbitals of the peripheral gold atoms corresponds to the polyhedron formed by the peripheral gold atoms. This arises from the sharper "focus" of the cylindrical seven-orbital spd^5 manifold of the peripheral gold atoms relative to the spherical four-orbital sp^3 and nine-orbital sp^3d^5 manifolds. Thus the number of positive eigenvalues of the graphs corresponding to the peripheral gold polyhedra relates to the number of bonding orbitals in the centered gold clusters.

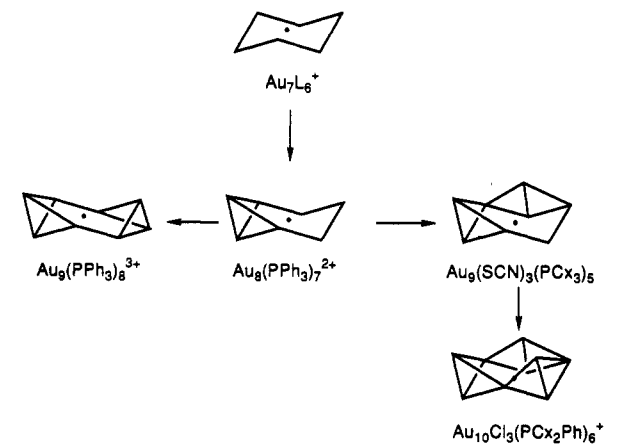

Figure 3. Structures of some toroidal gold clusters of the general formula $Au_nL_yX_{n-1-y}^{(y-5)+}$. The center gold atoms are shown by a dot (·).

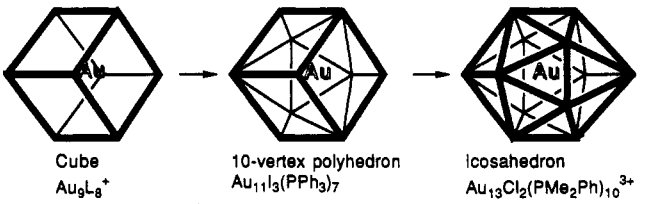

Figure 4. Structures of some spherical gold clusters of the general formula $Au_nL_yX_{n-1-y}^{(y-7)+}$. The center gold atoms are shown as Au.

(3) The center gold atom has 11 valence electrons. All but one of these electrons are needed to fill its five d orbitals. The remaining electron is in the spherically symmetric s orbital, which is the orbital of the center gold atom overlapping with the unique internal orbitals of the cylindrical spd^5 manifold of the peripheral gold atoms. This overlap lowers the energy of the lowest (fully symmetric) cluster bonding orbital without adding any new bonding orbitals. The center gold atom is therefore a donor of one skeletal electron.

(4) Mingos and co-workers[4] have observed a $12p + 16$ electron rule for toroidal centered gold clusters and a $12p + 18$ electron rule for spherical centered gold clusters where p $= n-1$ is the number of peripheral gold atoms. These numbers count not only the skeletal electrons but also the 10 electrons needed to fill the five d orbitals of each peripheral gold atom and the 2 electrons needed for one bond from each peripheral gold atom to an external L or X group. The $12p$ terms in Mingos' total electron numbers thus correspond to nonskeletal electrons involving only the peripheral gold atoms, leaving 16 or 18 electrons for a center gold atom with toroidal or spherical geometry, respectively. This corresponds exactly to the number of electrons required to fill the eight-orbital toroidal sp^2d^5 manifold or the nine-orbital spherical sp^3d^5 manifold, respectively. Subtracting 10 from the 16 or 18 electrons allocated to the center gold atom for its five d orbitals leaves 6 or 8 skeletal electrons for toroidal or spherical gold clusters, respectively.

(5) Consider L to be a two-electron donor ligand (e.g., tertiary phosphines or isocyanides) and X to be a one-electron donor ligand (e.g., halogen, pseudohalogen, $Co(CO)_4$, etc.). Then the above considerations give centered toroidal clusters (Figure 3) the general formula $Au_nL_yX_{n-1-n}^{(y-5)+}$ and centered spherical clusters (Figure 4) the general formula $Au_nL_yX_{n-1-y}^{(y-7)+}$.

All of the centered toroidal gold clusters depicted schematically in Figure 3 conform to the $Au_nL_yX_{n-1-y}^{(y-5)+}$ formula mentioned above. Thus the clusters $Au_7L_6^+$, $Au_8(PPh_3)_7^{2+}$,

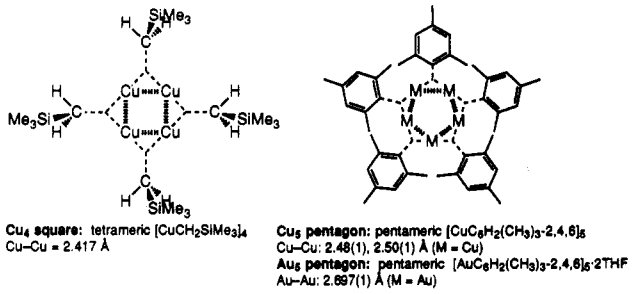

Figure 5. Structures of some copper alkyl and aryls with planar polygonal M_n units (n = 4 and 5).

$Au_9(PPh_3)_8^{3+}$, $Au_9(SCN)_3(PCx_3)_5$, and $Au_{10}Cl_3(PCx_2Ph)_6^+$ correspond to this formula with $n = 7$, $y = 6$; $n = 8$, $y = 7$; $n = 9$, $y = 8$; $n = 9$, $y = 5$; and $n = 10$, $y = 6$, respectively. The D_{2h} hexagonal belt cluster $Au_9(PPh_3)_8^{3+}$ and the C_{2v} hexagonal belt cluster $Au_9(SCN)_3(PCx_3)_5$ differ in the placement of the two distal gold atoms relative to the hexagonal belt, as depicted in Figure 3. The spectra of the graphs representing the interactions of the peripheral gold atoms in all of the toroidal clusters in Figure 3 have three positive eigenvalues in accord with the presence of three skeletal bonding orbitals corresponding to six skeletal electrons. Adding these six skeletal electrons to the 10 electrons required to fill the five d orbitals of the center gold atom gives the 16 electrons required to fill the eight-orbital sp^2d^5 manifold of the bonding orbitals of the center gold atom.

The three spherical gold clusters $Au_{13}Cl_2(PMe_2Ph)_{10}^{3+}$, $Au_{11}I_3(PPh_3)_7$, and $Au_9(PPh_3)_8^+$ depicted in Figure 4 all conform to the $Au_nL_yX_{n-1-y}^{(y-7)+}$ formula noted above with $n = 13$, $y = 10$; $n = 11$, $y = 7$; and $n = 9$, $y = 8$, respectively. The spectra of the graphs representing their peripheral gold atoms all have four positive eigenvalues in accord with the presence of four skeletal bonding orbitals corresponding to eight skeletal electrons. Addition of these eight skeletal electrons to the 10 electrons required to fill the five d orbitals of the center gold atom gives the 18 electrons required to fill the nine-orbital spherical sp^3d^5 manifold of the bonding orbitals of the center gold atom. The peripheral 10-vertex gold polyhedron in $Au_{11}I_3(PPh_3)_7$ can be formed from the peripheral gold icosahedron in $Au_{13}Cl_2(PMe_2Ph)_{10}^{3+}$ by the following two-step process: (1) removal of a triangular face, including its three vertices, its three edges, and the nine edges connecting this face with the remainder of the icosahedron, (2) addition of a new vertex in the location of the midpoint of the face that was removed followed by addition of three new edges to connect this new vertex to the degree 3 vertices of the nine-vertex icosahedral fragment produced in the first step. These processes preserve a C_3 axis of the icosahedron. Also application of this two-step process twice to an icosahedron so as to preserve a C_3 axis throughout the whole sequence of steps (Figure 4) leads to a cube such as the (distorted) cube found in $Au_9(PPh_3)_8^+$.[6] In this sense the 10-vertex peripheral gold polyhedron of $Au_{11}I_3(PPh_3)_7$ can be considered to be halfway between an icosahedron and a cube.

B. Coinage Metal Alkyls and Aryls. Coinage metal alkyls and aryls of the stoichiometry $(RM)_x$ (M = Cu, Ag; R = alkyl or aryl) clearly do not have simple monomeric structures with one-coordinating coinage metal atoms. Instead such alkyls have oligomeric structures (Figures 5–7), often with three-center M–C–M bonds analogous to the three-center Al–C–Al bonds in dimeric aluminum alkyls such as trimethylaluminum dimer. The bridging alkyl and aryl groups in these structures are donors of three apparent skeletal electrons. One of these three apparent skeletal electrons is a "real" electron arising from the carbon atom of the neutral alkyl or aryl group directly bonded to the two metal atoms through the three-center M–C–M bond. The other two apparent skeletal electrons are "virtual" electrons arising indirectly from the third atomic orbital in the three-center bond which otherwise would require an electron pair for the closed shell electronic configuration.

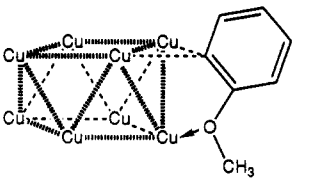

Figure 6. Cu_8 square antiprism in $[CuC_6H_4OMe\text{-}2]_8$ showing one of the eight 2-methoxyphenyl ligands.

Figure 5 depicts the structures of coinage metal alkyls with planar polygonal coinage metal rings M_n. The alkyl group in the tetrameric copper alkyl[14] $[CuCH_2SiMe_3]_4$ (Figure 5) can only bond to the copper atom through the alkyl carbon atom so that the Me_3SiCH_2 ligand is a monodentate ligand, although it bridges two copper atoms so that the cluster can be more precisely written $[Cu(CH_2SiMe_3)_{2/2}]_4$. The aryl group in the pentameric aryls[15] $[MC_6H_2Me_3\text{-}2,4,6]_5$ (Figure 5) is an analogous monodentate ligand so that these aryls can be written as $[M(C_6H_2Me_3\text{-}2,4,6)_{2/2}]_5$. Each coinage metal atom in the structures in Figure 5 can be considered to use a seven-orbital cylindrical spd^5 bonding orbital manifold with two linear sp hybrids. These linear sp hybrids form three-center two-electron Cu–C–Cu bonds with an alkyl or aryl carbon atom and an adjacent coinage metal atom. The two neutral bridging alkyl or aryl groups associated with each coinage metal atom formally donate a total of three apparent electrons (see above) so that each coinage metal atom has 11 + 3 = 14 valence electrons, which is exactly enough to fill its seven-orbital cylindrical spd^5 bonding manifold. The short metal–metal distances indicate appreciable metal–metal interactions in the coinage metal polygons in $[CuCH_2SiMe_3]_4$ and $[MC_6H_2Me_3\text{-}2,4,6]_5$ (Figure 5) in accord with $d\sigma \rightarrow p\sigma^*$ and $d\pi \rightarrow p\pi^*$ back-bonding into the coinage metal antibonding p orbitals not used for the cylindrical spd^5 bonding orbital manifold (Figure 2).

A related principle can be used to construct the octameric copper aryl $[CuC_6H_4OMe\text{-}2]_8$ (Figure 6).[16] In this case the copper atoms form a square antiprism. The 2-methoxyphenyl groups cap the eight triangular faces by forming three-center two-electron Cu–C–Cu bonds with two of the three copper vertices of the face being capped and a $CH_3O \rightarrow Cu$ dative bond with the third copper atom of the face so that each 2-methoxyphenyl group is shared with three copper atoms leading to the formulation $[Cu(C_6H_4OMe\text{-}2)_{3/3}]_8$. Each copper atom thus has a trigonal CuC_2O toroidal sp^2d^5 valence orbital manifold which is filled with 16 electrons as follows:

neutral copper atom	11 electrons
two bridging aryl groups	3 electrons
2-methoxy group lone pair	2 electrons
total electrons for a toroidal Cu atom	*16 electrons*

Each Cu_4 square face of the square antiprism in $[CuC_6H_4OMe\text{-}2]_8$ is closely related to the Cu_4 square in $[CuCH_2SiMe_3]_4$ discussed above. The ability of each of the eight 2-methoxyphenyl groups to function as a bidentate ligand bonding to metal atoms both through an aryl carbon and the methoxy oxygen acts as the "glue" to join two Cu_4 squares into the Cu_8 square antiprism in $[CuC_6H_4OMe\text{-}2]_8$. Bidentate aryl ligands are also found in the tetrameric $[CuC_6H_3(CH_2\text{-}$

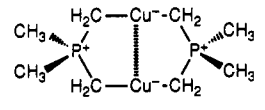

Dimeric
$[Cu(CH_2)_2P(CH_3)_2]_2$
Cu···Cu = 2.843(3) Å

Figure 7. Structure of the dimeric coinage metal alkyl $[Cu(CH_2)_2P(CH_3)_2]_2$.

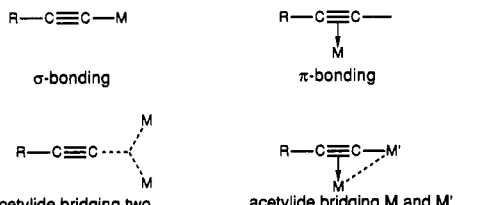

Figure 8. Bonding of an alkynyl (acetylide) ligand to one or two metal atoms.

NMe_2)-2-Me-5]$_4$ with a Cu_4 arrangement between square planar and tetrahedral.[17,18]

Another type of bidentate alkyl group is obtained by deprotonation of the phosphonium methylide $(CH_3)_3P{=}CH_2$ and occurs in the dimeric alkyl $[Cu(CH_2)_2P(CH_3)_2]_2$ (Figure 7).[19] In this structure each copper atom has a cylindrical spd^5 manifold with the linear sp hybrids forming two-center two-electron bonds with the alkyl carbons of two different $(CH_3)_2P(CH_2)_2$ groups. The cylindrical copper atoms obtain the 14 electrons required to fill the seven-orbital spd^5 manifold as follows:

neutral copper atom	11 electrons
two terminal alkyl groups: 2 × 1	2 electrons
negative charge on copper	1 electrons
total electrons for the cylindrical Cu atom	*14 electrons*

Note that each copper atom has a formal negative charge in $[Cu(CH_2)_2P(CH_3)_2]_2$, but these negative charges are balanced by formal positive charges on the phosphorus atoms so that $[Cu(CH_2)_2P(CH_3)_2]_2$ is a neutral molecule. The Cu–Cu distance in $[Cu(CH_2)_2P(CH_3)_2]_2$ is 2.843(3) Å indicative of $d\sigma \rightarrow p\sigma^*$ Cu–Cu bonding into the empty p* antibonding orbitals of the cylindrical copper atoms.

C. Coinage Metal Alkynyl Derivatives ("Acetylides). The coinage metals form a variety of alkynyl derivatives, most of which have oligomeric or polymeric structures. The terminal carbon atom of an alkynyl ligand, RC≡C–, has a σ-orbital which can form a two-electron two-center bond to a single metal atom or a two-electron three-center bond to a pair of metal atoms (Figure 8). Such σ-bond formation from a neutral alkynyl ligand results in the donation of a single electron to the metal atom. In addition, one of the two orthogonal π-orbitals can form a π-bond to a coinage metal atom. A neutral alkynyl ligand functions as a two-electron donor to the metal atom through such π-bonding. Alkynyl ligands can bridge a pair of coinage metal atoms either by forming a two-electron three-center CM_2 bond with a pair of metal atoms using the carbon σ-orbital or by forming a σ-bond with one metal atom and a π-bond with another metal atom using both a C≡C π-orbital and the carbon σ-orbital (Figure 8). Both homometallic and heterometallic coinage metal acetylides are known.

Figure 9 depicts the structure of two phenylethynylcopper derivatives. Polymeric $[CuC_2C_6H_5]_n$ has an infinite zigzag chain of copper atoms with Cu–Cu bonding distances of 2.42–

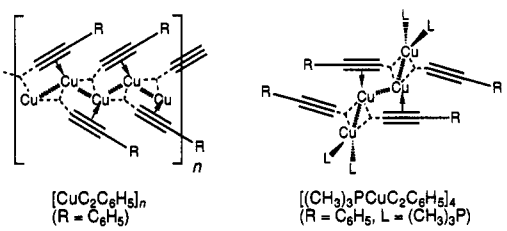

Figure 9. Structures of some phenylethynylcopper derivatives.

2.47 Å (hashed lines in Figure 9). The phenylethynyl ligands bridge three copper atoms, two through the formation of a three-center two-electron CCu_2 bond (dashed lines in Figure 9) and the third through an alkynyl–Cu π-bond (arrows in Figure 9). Each copper atom has an eight-orbital toroidal sp^2d^5 manifold with trigonal sp^2 hybrids. Two of the trigonal sp^2 hybrids are used to form the two three-center CCu_2 bonds with the adjacent phenylethynyl ligands, whereas the third copper trigonal sp^2 hybrid overlaps with a carbon–carbon π-bonding orbital of a third phenylethynyl ligand. Each copper atom has a total of 16 valence electrons to fill its eight-orbital toroidal sp^2d^5 manifold as follows:

neutral copper atom	11 electrons
3-center bonds to two phenylethynyl groups	3 electrons
one π-bond to the C≡C of a phenylethynyl group	2 electrons
total electrons for the toroidal Cu atom	*16 electrons*

Complexation of phenylethynylcopper with trimethylphosphine reduces its degree of aggregation to that of a tetramer $[(CH_3)_3PCuC_2C_6H_5]_4$ (Figure 9)[20] containing a four-copper fragment of the zigzag chain found in $[CuC_2C_6H_5]_n$. Each end copper atom bears two trimethylphosphine ligands (L in Figure 9) and has tetrahedral coordination with a nine-orbital spherical sp^3d^5 manifold and the 18-electron noble gas configuration as follows:

neutral copper atom	11 electrons
2 $(CH_3)_3$ P ligands: 2 × 2	4 electrons
3-center bonds to two phenylethynyl groups	3 electrons
total electrons for the end (spherical) Cu atom	*18 electrons*

The middle copper atoms have eight-orbital toroidal sp^2d^5 manifolds and trigonal planar coordination each forming two three-center σ-bonds to adjacent phenylethynyl groups and a third bond to a π-orbital of another phenylethynyl group. The middle copper atoms have the 16 valence electrons required to fill their eight-orbital toroidal sp^2d^5 manifolds as follows:

neutral copper atom	11 electrons
3-center bonds to two phenylethynyl groups	3 electrons
one π-bond to the C≡C of a phenylethynyl group	2 electrons
total electrons for the middle (toroidal) Cu atom	*16 electrons*

Note that in $[(CH_3)_3PCuC_2C_6H_5]_4$ only two of the four phenylethynyl ligands are π-bonded to metal atoms (Figure 9).

The phenylethynylsilver derivative[21] $[(CH_3)_3PAgC_2C_6H_5]_n$ (Figure 10) is polymeric in contrast to its tetrameric copper analogue (Figure 9). A characteristic feature of $[(CH_3)_3PAgC_2C_6H_5]_n$ is the presence of silver atoms of two types, namely, $[(CH_3)_3P]_2Ag^+$ units with formal positive charges and $(C_6H_5C{\equiv}C)_2Ag^-$ units with formal negative charges. The silver compound can be formulated as an infinite straight chain of approximately square planar silver atoms with eight-orbital toroidal sp^2d^5 valence orbital manifolds and two-center two-electron Ag–Ag bonds. Each type of silver atom has a total of the 16 valence electrons required to fill its eight-orbital toroidal sp^2d^5 manifold, i.e.

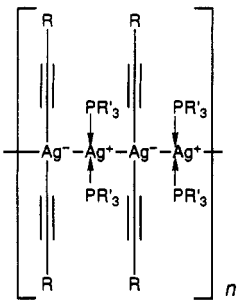

$[(CH_3)_3PAgC_2C_6H_5]_n$
(R = C_6H_5, R' = CH_3)
Ag···Ag = 3.033 Å

Figure 10. Phenylethynylsilver derivative $[(CH_3)_3PAgC_2C_6H_5]_n$.

	$(Me_3P)_2Ag^+$ unit	$(PhC_2)_2Ag^-$ unit
neutral silver atom	11 electrons	11 electrons
two Ag–Ag bonds to adjacent Ag atoms: 2 × 1	2 electrons	2 electrons
two $(CH_3)_3P$ ligands: 2 × 2	4 electrons	
two σ-bonds to $C_6H_5C{\equiv}C$–ligands: 2 × 1		2 electrons
formal charge	(+) –1 electron	(–) 1 electron
total electrons for the toroidal Ag atoms	*16 electrons*	*16 electrons*

An equivalent model for $[(CH_3)_3PAgC_2C_6H_5]_n$ can be derived by using linear two-coordinate $[(CH_3)_3P]_2Ag^+$ and $(C_6H_5C{\equiv}C)_2Ag^-$ building blocks with seven-orbital cylindrical spd^5 manifolds. The silver–silver bonding would then be of the $d\sigma \rightarrow p\sigma^*$ type (Figure 2) involving electron donation from filled d orbitals on one silver atom into empty p orbitals on an adjacent silver atom. This removes the silver–silver bonding electrons from the silver valence orbital manifolds so that both types of cylindrical silver atoms, namely, those in the $[(CH_3)_3P]_2Ag^+$ units and the $(C_6H_5C{\equiv}C)_2Ag^-$ units, have the 14 valence electrons required to fill the seven-orbital cylindrical spd^5 bonding orbital manifolds.

Mixed coinage metal alkynyl clusters (Figures 11 and 12) can be constructed by using linear $RC{\equiv}C{-}M^-{-}C{\equiv}R$ units with a negative formal charge on the coinage metal atom and linear L_2M^+ or toroidal L_3M^+ units with a positive formal charge on the coinage metal atom (L = electron pair from a $C{\equiv}C$ π-orbital or a trivalent phosphorus ligand). The metal–metal bonding in these structures then arises from the $d\sigma \rightarrow p\sigma^*$ bonding (Figure 2) from filled d orbitals on one coinage metal atom into empty p orbitals on an adjacent coinage metal atom. In the neutral cluster $[(C_6H_5)_3P]_2Ag_2Au_2(C_2C_6H_5)_4$ (Figure 11)[22] there is an Ag_2Au_2 rhombus in which the silver atoms have eight-orbital sp^2d^5 toroidal manifolds with trigonal planar sp^2 coordination and the gold atoms have seven-orbital spd^5 cylindrical manifolds with linear sp coordination. In the anionic cluster (Figure 11)[23] $[Au_3Cu_2(C_2C_6H_5)_6]^-$ there is a Au_3Cu_2 trigonal bipyramid in which the copper atoms have eight-orbital sp^2d^5 toroidal manifolds with trigonal planar sp^2 coordination and the gold atoms have seven-orbital spd^5 cylindrical manifolds with linear sp coordination. Thus both of these clusters have formally positive toroidal three-coordinate trigonal planar metals and formally negative cylindrical linear two-coordinate metals. All of the metal atoms have exactly the number of valence electrons required to fill their valence orbital manifolds, namely, 14 for the metals with seven-orbital spd^5 cylindrical bonding manifolds and 16 for the metals with eight-orbital sp^2d^5 toroidal bonding manifolds.

The most complicated mixed coinage metal alkynyl cluster that has been characterized by X-ray diffraction is the anionic cluster $[(RC_2)_2Cu\{Ag_2[Cu(C_2R)_2]_2\}_3]^-$ (R = C_6H_5; Figure 12) which contains a total of 13 coinage metal atoms.[24,25] The

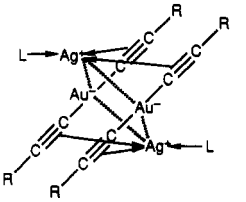

$L_2Ag_2Au_2(C_2R)_4$
Ag_2Au_2 rhombus

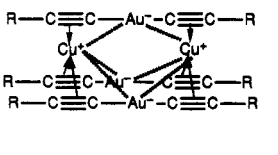

$[Au_3Cu_2(C_2R)_6]^-$
Au_3Cu_2 trigonal bipyramid

Figure 11. Some mixed coinage metal alkynyls.

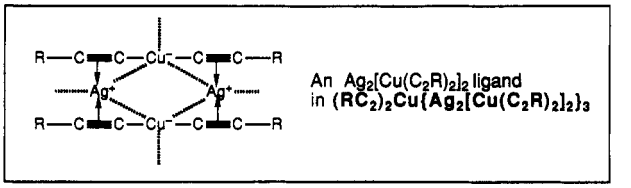

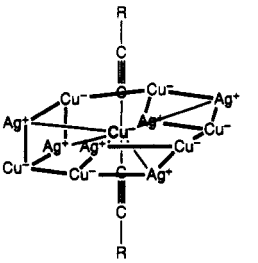

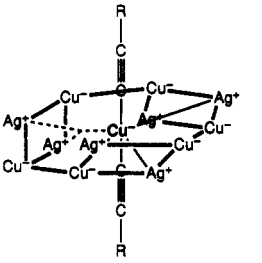

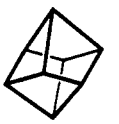

8-coordinate central Cu
All 2c–2e bonds
D_{3d} distorted cube
"Forbidden polyhedron"
***f* orbitals required!**

7-coordinate central Cu
One 3c-2e bond
Six 2c-2e bonds
D_{5h} pentagonal bipyramid

Figure 12. Structure and bonding in the 13-atom heterometallic coinage metal alkynyl cluster $[(RC{\equiv}C)_2Cu\{Ag_2[Cu(C_2R)_2]_2\}_3]^-$.

structure of this cluster contains one central and six peripheral linear $C_6H_5C{\equiv}C{-}Cu^-{-}C{\equiv}CC_6H_5$ units with formal negative charges on each central copper atom. The triple bonds of the peripheral $C_6H_5C{\equiv}C{-}Cu^0{-}C{\equiv}CC_6H_5$ units are π-bonded to the silver atoms to give linear $(\pi\text{-alkyne})_2Ag^+$ units with formal positive charges on each central silver atom. The central coinage metals in both the negative $C_6H_5C{\equiv}C{-}Cu^-{-}C{\equiv}CC_6H_5$ units and the positive $(\pi\text{-alkyne})_2Ag^+$ units have the 14 valence electrons required for their cylindrical spd^5 valence orbital manifolds. The formal negative charges on the seven copper atoms and formal positive charges on the six silver atoms lead to the observed –1 charge on the ion. The peripheral $C_6H_5C{\equiv}C{-}Cu^-{-}C{\equiv}CC_6H_5$ and $(\pi\text{-alkyne})_2Ag^+$ units combine to form three Cu_2Ag_2 neutral rhombus ligands which surround the central copper atom.

In $[(RC_2)_2Cu\{Ag_2[Cu(C_2R)_2]_2\}_3]^-$ the topology of the central copper coordination can be derived from a cube distorted to D_{3d} symmetry with the phenylethynyl ligands bonded to the central copper atom located along the C_3 axis (Figure 12) and in that sense is related to the D_3 distortion of the cube in the centered gold cluster $Au_9(PPh_3)_8^+$. All 10 electrons of the central copper(I) atom are involved in $d\sigma \rightarrow p\sigma^*$ or $d\pi \rightarrow p\pi^*$ dative bonding (Figure 2) to empty p antibonding orbitals of the six silver atoms but one three-center Ag–Cu–Ag bond is necessary since there are only five copper(I) electron pairs but six silver atoms providing empty orbitals. In addition, the D_{3d} distorted cubic coordination of

Table I. Mercury–Mercury Bond Distances

compound	Hg–Hg (Å)
Hg metal	3.00, 3.47
Hg_2F_2	2.43
Hg_2Cl_2	2.45
Hg_2Br_2	2.50
Hg_2I_2	2.69
$Hg_3(AsF_6)_2$	2.552(4)
$Hg_3(AlCl_4)_2$	2.56
$Hg_4(AsF_6)_2$	2.70 (inner), 2.57 (outer)
$Hg_{2.83}(AsF_6)$	2.64(1)
$Na_3Hg(Hg_6^{4-})$	2.99
NaHg	3.05, 3.05, 3.22
KHg	3.02, 3.04, 3.36
CsHg	3.00, 3.02
$NaHg_2$	2.90, 3.23
KHg_2	3.00, 3.02, 3.08
$[HgOs_3(CO)_{11}]_3$	3.122(3), 3.082(3), 3.097(3)
$[HgMn(CO)_2C_5H_4Me]_4$	2.888(2)
$Hg_6\{Pt[Pr^i_2P(CH_2)_4PPr^i_2]\}_4$	3.087(2), 3.080(2), 3.224(2), 3.268(2), 3.275(2)
$Hg_2[Pt_3(\mu_2\text{-}CO)_3(PPhPr^i_2)_3]_2$	3.225(1)

the central copper atom requires sp^3d^3f rather than sp^3d^4 hybridization because of the presence of an inversion center in D_{3d} symmetry.[26] The coordination of the central copper atom in $[(RC_2)_2Cu\{Ag_2[Cu(C_2R)_2]_2\}_3]^-$ can be regarded as a distorted pentagonal bipyramid with bonds to carbon atoms in the phenylethynyl ligands in the axial positions and bonds to silver atoms in the equatorial positions.

MERCURY CLUSTERS

A. Mercury–Mercury Distances as Indications of Bond Type. The mercury–mercury distances in polynuclear mercury derivatives (Table I) provide an excellent indication as to the nature of mercury–mercury interactions. In true "mercurous" Hg_2^{2+} derivatives as well as similar derivatives of longer linear mercury chains (e.g., Hg_3^{2+}, Hg_4^{2+}) the Hg–Hg distances fall in the range 2.4–2.7 Å, indicative of strong primary covalent bonding arising from overlap of linear sp hybrid orbitals.[27-29] In cases where the primary mercury bonding is diverted to other atoms, such as transition metal atoms in metal clusters, the Hg–Hg distances increase to the range 2.9–3.2 Å, indicating the presence of only secondary mercury–mercury bonding (Table I).

B. Alkali Metal Amalgams. Several alkali metal amalgams have been structurally characterized including the sodium amalgams[30] $NaHg_2$, NaHg, and Na_3Hg_2, the potassium amalgams[31] KHg_2 and KHg, the rubidium amalgam[32] $Rb_{15}Hg_{16}$, and the cesium amalgam[33] CsHg. The most highly reduced of these species, namely, Na_3Hg_2, has been shown[34] to contain discrete 2.99-Å square planar Hg_4^{6-} clusters which are *not* isoelectronic with other square planar posttransition metal clusters such as Bi_4^{2-}, Se_4^{2+}, and Te_4^{2+}. In gold-colored NaHg slightly distorted 3.05 × 3.22 Å Hg_4 rectangles are fused into a zigzag ribbon, whereas, in the likewise gold-colored KHg, slightly distorted (93.5° rather than 90°) 3.03-Å Hg_4 squares are linked by 3.36-Å Hg–Hg bonds. The structure of $Rb_{15}Hg_{16}$ has Hg_8 cubes (Hg–Hg edges in the range 2.95–3.04 Å). More complicated networks of mercury rectangles and parallelograms are present in $NaHg_2$ and KHg_2. Thus the prototypical building blocks for alkali metal amalgams are derived from the Hg_4^{6-} squares found in Na_3Hg_2. Electrochemical studies[35,36] suggest that similar mercury cluster anions are present in "quaternary ammonium amalgams", although difficulties in obtaining crystals from these air- and moisture-sensitive systems have precluded their definitive structural characterization.

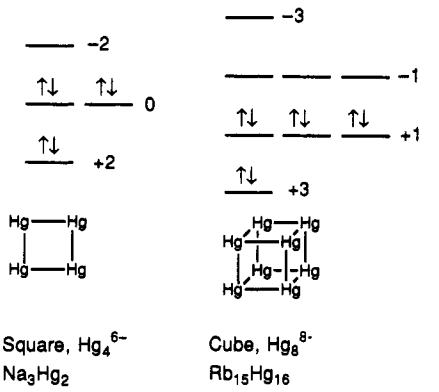

Figure 13. Spectra of the square found in the Hg_4^{6-} anion in Na_3Hg_2 and the cube found in the Hg_8^{8-} anion in $Rb_{15}Hg_{16}$.

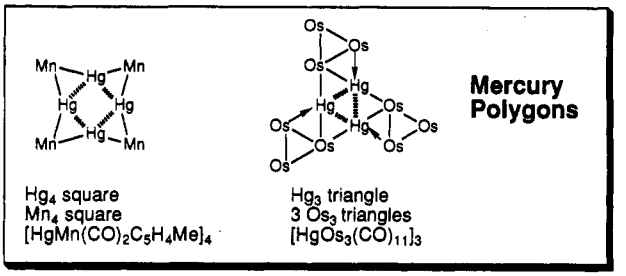

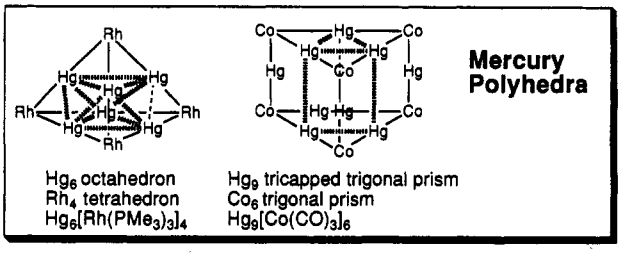

Figure 14. Transition metal clusters containing mercury polygons or mercury polyhedra. Some of the edges of the Hg_9 tricapped trigonal prism are omitted for clarity in $Hg_9[Co(CO)_3]_6$.

The mercury atoms in anionic mercury clusters such as those found in alkali metal amalgams can be considered to have seven-orbital spd^5 cylindrical bonding manifolds similar to the vertex gold atoms in the peripheral polyhedra of the centered gold clusters. Six of these seven orbitals, namely, the s orbital and the five d orbitals, are external orbitals, whereas the single p orbital is an internal orbital. The chemical bonding topology of the mercury atoms in anionic mercury clusters can be related to the spectrum of the graph describing the topology of the overlap of these internal orbitals. Thus the mercury square found in Na_3Hg_2 has one positive eigenvalue and two zero eigenvalues, whereas the cube found in $Rb_{15}Hg_{16}$ has four positive eigenvalues (Figure 13).

Consider first the mercury square found in the Hg_4^{6-} anion of Na_3Hg_2. Since a neutral mercury atom with six external orbitals for its 12 valence electrons is a donor of zero skeletal electrons, the Hg_4^{6-} anion has only the six skeletal electrons arising from the 6– charge. These six skeletal electrons are exactly enough electrons to fill the single bonding and two nonbonding orbitals of the mercury square, as indicated in Figure 13. Similarly, each mercury cube in the "mercubane" cluster $Rb_{15}Hg_{16}$ has a 7.5 skeletal electrons which is only 0.5 skeletal electron short of the eight skeletal electrons required to fill all four of its bonding orbitals (Figure 13).

C. Mercury Vertices in Transition Metal Clusters. Transition metal clusters containing mercury vertices[37] can be classified into two types: two-dimensional clusters (Figure 14, top) in which the mercury atoms form a polygon such as

Table II. Smallest Members of the Homologous Series of Clusters $[Hg_3(ML_3)_2]_x$ Consisting of a Mercury Polyhedron Inside a Transition Metal Macropolyhedron

x	symmetry	type	v	e	f	type	v	e	f	example
2	T_d	octahedron	6	12	8	tetrahedron	4	6	4	$Hg_6[Rh(PMe_3)_3]_4$
3	D_{3h}	tricapped trigonal prism	9	21	14	trigonal prism	6	9	5	$Hg_9[Co(CO)_3]_6$
4	O_h	cuboctahedron	12	24	14	cube	8	12	6	

a triangle in $[HgOs_3(CO)_{11}]_3$ [38] or a square in $[HgMn(CO)_2C_5H_4Me]_4$ [39] and three-dimensional clusters (Figure 14, bottom) in which the mercury atoms form a polyhedron such as an octahedron in $Hg_6[Rh(PMe_3)_3]_4$ [4] or $Hg_6\{Pt[Pr^i_2P(CH_2)_4PPr^i_2]\}_4$ [41] or a tricapped trigonal prism in $Hg_9[Co(CO)_3]_6$[42]. Transition metal clusters containing mercury polygons (Figure 14, top) arise from bifunctional transition metal fragments such as $Fe(CO)_4$ and $CpMn(CO)_2$ (Cp = cyclopentadienyl or substituted cyclopentadienyl), leading to degree two vertices in the large transition metal macropolygon. Transition metal clusters containing mercury polyhedra arise from trifunctional transition metal fragments such as $Co(CO)_3$ and $Rh(PR_3)_3$, leading to degree three vertices in the large transition metal macropolyhedron. The graph of the polygon or polyhedron formed by the mercury vertices is thus the line graph[43] of the graph of the polygon or polyhedron formed by the transition metal vertices.

Combinations of difunctional transition metal vertices with mercury vertices lead to clusters with equal numbers of transition metal and mercury vertices consisting of a mercury polygon within a transition metal macropolygon (Figure 14, top). The bond angles at the transition metal vertices determine the sizes of the polygons, with squares apparently being preferred as is the case with alkali metal amalgams (Figure 13). An example of a structurally characterized cluster of this type is $[HgMn(CO)_2C_5H_4Me]_4$. The Mn–Hg–Mn edges of the Mn_4 macrosquare in $[HgMn(CO)_2C_5H_4Me]_4$ are bent inward toward the center of the square in accord with secondary mercury–mercury bonding, leading to 2.888(2)-Å Hg–Hg bond distances. A similar structure can be postulated for the long-known[44] but insoluble $[HgFe(CO)_4]_4$ on the basis of its similar infrared spectrum to the structurally characterized[45] $[CdFe(CO)_4]_4 \cdot 2Me_2CO$.

Combinations of trifunctional transition metal vertices with mercury vertices lead to clusters having a mercury polyhedron within a transition metal macropolyhedron (Figure 14, bottom). Most known examples of such clusters have trifunctional transition metal vertices of the type ML_3 (M = Co, Rh, Ir; L = CO, R_3P). The number of mercury atoms in such clusters is equal to the number of edges in the transition metal macropolyhedron. If this macropolyhedron has m vertices, all of degree 3 implied by the trifunctionality of the transition metal units at the vertices, then there are $^3/_2m$ M–Hg–M edges, and such clusters have the overall stoichiometry $[Hg_3(ML_3)_2]_x$. Table II lists the properties of the first three members of this homologous series for which both the mercury polyhedron and the transition metal macropolyhedron are readily recognizable polyhedra.

A platinum–mercury cluster that has a structure intermediate between square derivatives such as $[HgMn(CO)_2C_5H_4Me]_4$ and tetrahedral derivatives such as $Hg_6[Rh(PMe_3)_3]_4$ is $Hg_6[Pt(dipb)]_4$ (Figure 15: 2L = dipb = $Ph_2P(CH_2)_4PPh_2$). A square structure is first constructed by using four of the six mercury atoms and all four platinum atoms with a sp^2d^5 toroidal manifold for the square planar platinum atoms. The empty antibonding p_z orbitals of the four square planar platinum atoms can then overlap with the filled s orbitals of the fifth and sixth mercury atoms in two-electron three-center

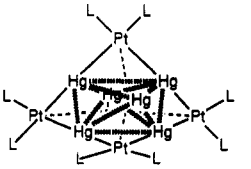

Figure 15. Structure of $Hg_6[Pt(dipb)]_4$ (2L = dipb = $Ph_2P(CH_2)_4PPh_2$).

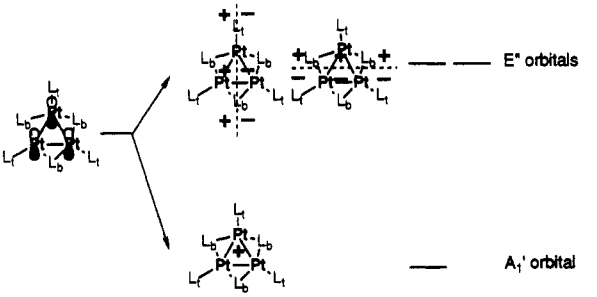

Figure 16. Neutral Pt_3L_6 unit and the interaction of its empty p_z orbitals in C_3 (triangular) topology. The molecular orbital labels correspond to D_{3h} symmetry. Nodes of the E′ orbitals are indicated by dotted lines.

Pt_2Hg bonds. These three-center bonds lead to considerable distortion of the original Pt_4 macrosquare toward a macrotetrahedron like the Rh_4 macrotetrahedron in $Hg_6[Rh(PMe_3)_3]_4$. However, $Hg_6[Pt(dipb)]_4$ has four less skeletal electrons than $Hg_6[Rh(PMe_3)_3]_4$. The topology of the six mercury atoms in $Hg_6[Pt(dipb)]_4$ is that of an octahedron like that of the six mercury atoms in $Hg_6[Rh(PMe_3)_3]_4$ despite the difference in skeletal electron counts.

D. Mercury Atoms Sandwiched between Pt_3 Triangles. Ideas related to those discussed above are involved in the interaction of mercury atoms with palladium and platinum triangle clusters to form sandwich compounds in which one or two mercury atoms are sandwiched between two Pt_3 or Pd_3 triangles.[46–48] The building blocks of such clusters (Figure 16) consist of triangular M_3L_6 (M = Pd, Pt) units in which three of the six L ligands are terminal (L_t) and the other three L ligands (L_b) bridge the three triangle edges. The metal atoms thus have eight-orbital sp^2d^5 toroidal manifolds with planar pentagonal $sp^2(x,y)d^2(xy,x^2-y^2)$ hybridization. The empty p_z orbitals outside the sp^2d^5 bonding manifolds can overlap with triangular C_3 (or K_3) topology similar to the p_z orbitals in the cyclopropenium cation, $C_3H_3^+$, to form an A_1' orbital with no nodes perpendicular to the plane of the Pt_3 triangle and two degenerate orthogonal E″ orbitals with one node each perpendicular to the plane of the Pt_3 triangle (Figure 16). Filling the A_1' orbital with an electron pair to form the dianion $M_3L_6^{2-}$ leads to a π-electron configuration similar to that of the cyclopropenium cation.

The Pt_3L_6 units can combine with mercury atoms to form two types of clusters (Figure 17), namely, $(Pt_3)Hg(Pt_3)$ sandwiches containing one mercury atom such as the isocyanide complex $Hg[Pt_3(\mu_2\text{-}2,6\text{-}Me_2C_6H_3NC)_3(2,6\text{-}Me_2C_6H_3NC)_3]_2$ [49] and carbonyl derivatives $Hg[Pt_3(\mu_2\text{-}CO)_3L_3]_2$ (L = Pr^i_3P and Bu^tEt_2P) and the diamagnetic sandwich $Hg_2[Pt_3(\mu_2\text{-}CO)_3L_3]_2$ (L = Pr^i_2PhP),[50] containing a pair of mercury atoms sandwiched between the two Pt_3 triangles.

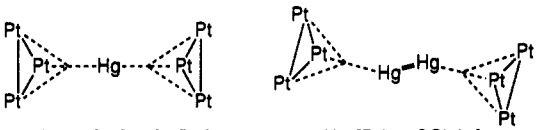

Figure 17. Metal frameworks of $Hg(Pt_3)_2$ and $(Pt_3)Hg–Hg(Pt_3)$ sandwich clusters. The Hg–Hg $d\sigma \rightarrow p\sigma^*$ bonding is shown by a dashed line.

The mercury atom in clusters of the type $Hg[Pt_3L_6]_2$ can bond to the two Pt_3 triangles by overlap of two filled mercury linear hybrid orbitals each with an empty anodal A_1' molecular orbital formed by the interaction of the empty p_z orbitals in a Pt_3L_6 unit (Figure 16). In addition Hg → Pt dative $d\pi \rightarrow p\pi^*$ bonding is possible by overlap of the filled mercury d_{xz} and d_{yz} orbitals with the empty uninodal E″ molecular orbitals from the Pt_3L_6 unit (Figure 16).

In the dimercury cluster $Hg_2[Pt_3(\mu_2\text{-}CO)_3(PPhPr^i_2)_3]_2$ (Figure 17) the large Hg–Hg distance of 3.225(1) Å indicates that this cluster is not a "mercurous" Hg_2^{2+} compound in which the Hg–Hg distance would be expected to be in the much smaller range 2.4–2.7 Å. In addition, formulation of $Hg_2[Pt_3(\mu_2\text{-}CO)_3(PPhPr^i_2)_3]_2$ as a Hg_2^{2+} compound would require the $Pt_3(\mu_2\text{-}CO)_3(PPhPr^i_2)_3$ units at each end of the molecule to be monoanions which would make them paramagnetic, in apparent disagreement with the observed diamagnetism of this compound. For these reasons the Hg–Hg bond in $Hg_2[Pt_3(\mu_2\text{-}CO)_3(PPhPr^i_2)_3]_2$ is considered to be another example of the $d\sigma \rightarrow p\sigma^*$ bonding discussed extensively in this paper. The stability of $Hg_2[Pt_3(\mu_2\text{-}CO)_3(PPhPr^i_2)_3]_2$, the two halves of which are held together solely by the Hg–Hg $d\sigma \rightarrow p\sigma^*$ bonding, indicates that such bonding in the heavy elements can be reasonably strong.

REFERENCES AND NOTES

(1) Nyholm, R. S. *Proc. Chem. Soc.* **1961**, 273.
(2) Dedieu, A.; Hoffmann, R. *J. Am. Chem. Soc.* **1978**, *100*, 2074.
(3) King, R. B. *Inorg. Chim. Acta* **1986**, *116*, 109.
(4) Briant, C. E.; Hall, K. P.; Wheeler, A. C.; Mingos, D. M. P. *Chem. Commun.* **1984**, 248.
(5) King, R. B. *Prog. Inorg. Chem.* **1972**, *15*, 287.
(6) van der Linden, J. G. M.; Paulissen, M. L. H.; Schmitz, J. E. J. *J. Am. Chem. Soc.* **1983**, *105*, 1903.
(7) Briant, C. E.; Theobald, B. R. C.; White, J. W.; Bell, L. K.; Mingos, D. M. P.; Welch, A. J. *Chem. Commun.* **1981**, 201.
(8) King, R. B.; Rouvray, D. H. *J. Am. Chem. Soc.* **1977**, *99*, 7834.
(9) King, R. B. In *Chemical Applications of Topology and Graph Theory*; King, R. B., Ed.; Elsevier: Amsterdam, 1983; pp 99–123.
(10) King, R. B. In *Molecular Structures and Energetics*; Liebman, J. F., Greenberg, A., Eds.; VCH Publishers: Deerfield Beach, FL, 1986; pp 123–148.
(11) King, R. B. *J. Math. Chem.* **1987**, *1*, 249.
(12) King, R. B. *Isr. J. Chem.* **1990**, *30*, 315.
(13) King, R. B. *Applications of Graph Theory and Topology in Inorganic Cluster and Coordination Chemistry*; CRC Press: Boca Raton, FL, 1993; Chapter 4.
(14) Jarvis, J. A. J.; Pearce, R.; Lappert, M. F. *J. Chem. Soc., Dalton Trans.* **1977**, 999.
(15) Meyer, E. M.; Gambarotta, S.; Floriani, C.; Chiesi-Villa, A.; Guastini, C. *Organometallics* **1989**, *8*, 1067.
(16) Camus, A.; Marsich, N.; Nardin, G.; Randaccio, L. *J. Organomet. Chem.* **1979**, *174*, 121.
(17) van Koten, G.; Noltes, J. G. *J. Organomet. Chem.* **1975**, *84*, 129.
(18) Guss, J. M.; Mason, R.; Søtofte, A. I.; van Koten, G.; Noltes, J. G. *Chem. Commun.* **1972**, 446.
(19) Nardin, G.; Randaccio, L.; Zangrando, E. *J. Organomet. Chem.* **1974**, *74*, C23.
(20) Corfield, P. W. R.; Shearer, H. M. M. *Acta Crystallogr.* **1966**, *21*, 957.
(21) Corfield, P. W. R.; Shearer, H. M. M. *Acta Crystallogr.* **1966**, *20*, 502.
(22) Abu-Salah, O. M. *J. Organomet. Chem.* **1990**, *387*, 123.
(23) Abu-Salah, O. M.; Al-Ohaly, A. A.; Knobler, C. B. *Chem. Commun.* **1985**, 1502.
(24) Abu-Salah, O. M.; Hussain, M. S.; Schlemper, E. O. *Chem. Commun.* **1988**, 212.
(25) Hussain, M. S.; Abu-Salah, O. M. *J. Organomet. Chem.* **1993**, *445*, 295.
(26) King, R. B. *Theor. Chim. Acta* **1984**, *64*, 453.
(27) Grdenić, D. *Q. Rev.* **1965**, *19*, 303.
(28) Roberts, H. L. *Adv. Inorg. Chem. Radiochem.* **1968**, *11*, 309.
(29) Gillespie, R. J.; Passmore, J. *Adv. Inorg. Chem. Radiochem.* **1975**, *17*, 49.
(30) Nielsen, J. W.; Baenziger, N. C. *Acta Crystallogr.* **1954**, *7*, 277.
(31) Duwell, E. J.; Baenziger, N. C. *Acta Crystallogr.* **1955**, *8*, 705.
(32) Deiseroth, H.-J.; Strunck, A. *Angew. Chem., Int. Ed. Engl.* **1989**, *28*, 1251.
(33) Deiseroth, H.-J.; Strunck, A. *Angew. Chem., Int. Ed. Engl.* **1987**, *26*, 687.
(34) Corbett, J. D.; *Inorg. Nucl. Engl. Chem. Lett.* **1969**, *5*, 81.
(35) Garcia, E.; Cowley, A. H.; Bard, A. J. *J. Am. Chem. Soc.* **1986**, *108*, 6082.
(36) Kariv-Miller, E.; Svetličić, V. *J. Electroanal. Chem.* **1986**, *205*, 319.
(37) King, R. B. *Polyhedron* **1988**, *7*, 1813.
(38) Fajardo, M.; Holden, H. D.; Johnson, B. F. G.; Lewis, J.; Raithby, P. R. *Chem. Commun.* **1984**, 24.
(39) Gäde, W.; Weiss, E. *Angew. Chem., Int. Ed. Engl.* **1981**, *20*, 803.
(40) Jones, R. A.; Real, F. M.; Wilkinson, G.; Galas, A. M. R.; Hursthouse, M. B. *J. Chem. Soc., Dalton Trans.* **1981**, 126.
(41) Wurst, K.; Strähle, J. *Z. Anorg. Allg. Chem.* **1991**, *595*, 239.
(42) Ragosta, J. M.; Burlitch, J. M. *Chem. Commun.* **1985**, 1187.
(43) Biggs, N. L. *Algebraic Graph Theory*; Cambridge University Press: London, 1974; p 17.
(44) Hock, H.; Stuhlmann, H. *Chem. Ber.* **1929**, *62*, 431.
(45) Ernst, R. D.; Marks, T. J.; Ibers, J. A. *J. Am. Chem. Soc.* **1977**, *99*, 2090.
(46) Mealli, C. *J. Am. Chem. Soc.* **1985**, *107*, 2245.
(47) Underwood, D. J.; Hoffmann, R.; Tatsumi, K.; Nakamura, A.; Yamamoto, Y. *J. Am. Chem. Soc.* **1985**, *107*, 5968.
(48) Puddephatt, R. J.; Manojlovic-Muir, L.; Muir, K. W. *Polyhedron* **1990**, *9*, 2767.
(49) Yamamoto, Y.; Yamazaki, H.; Sakurai, T. *J. Am. Chem. Soc.* **1982**, *104*, 2329.
(50) Albinati, A.; Moor, A.; Pregosin, P. S.; Venanzi, L. M. *J. Am. Chem. Soc.* **1982**, *104*, 7672.